

Analysing surveys of our Galaxy I: basic astrometric data

Paul J. McMillan^{1*} and James Binney¹

¹ *Rudolf Peierls Centre for Theoretical Physics, Keble Road, Oxford OX1 3NP, UK*

September 20, 2011

ABSTRACT

We consider what is the best way to extract science from large surveys of the Milky Way galaxy. The diversity of data gathered in these surveys, together with our position within the Galaxy, imply that science must be extracted by fitting dynamical models to the data in the space of the observables. Models based on orbital tori promise to be superior for this task than traditional types of models, such as N-body models and Schwarzschild models. A formalism that allows such models to be fitted to data is developed and tested on pseudodata of varying richness drawn from axisymmetric disc models.

Key words: galaxies: evolution – galaxies: kinematics and dynamics – Galaxy: disc – solar neighbourhood – methods: data analysis

1 INTRODUCTION

A major thread of current research is work directed at understanding the origin of galaxies. There are excellent prospects of achieving this goal by combining endeavours in three distinct areas: observations of galaxy formation taking place at high redshift, numerical simulations of the gravitational aggregation of dark matter and baryons, and studies of the Milky Way. The latter field is dominated by a series of major observational programs that started fifteen years ago with ESA’s Hipparcos mission, which returned parallaxes and proper motions for $\sim 10^5$ stars (Perryman 1997). Hipparcos established a more secure astrometric reference frame, and the UCAC-3 catalogue (Zacharias et al. 2010) uses this frame to give proper motions for several million stars. These enhancements of our astrometric database have been matched by the release of major photometric catalogues DENIS (Epchtein et al. 2005), 2MASS (Skrutskie et al. 2006), SDSS (Abazajian 2009), SEGUE (Yanny et al. 2009), and the accumulation of enormous numbers of stellar spectra, starting with the Geneva–Copenhagen survey (Nordström et al. 2004; Holmberg et al. 2007, hereafter GCS) and continuing with the SDSS, SEGUE and RAVE (Steinmetz et al. 2006; Siebert et al. 2011) surveys. Major programs to obtain low-dispersion stellar spectra are currently underway – on completion the SEGUE and RAVE surveys will each provide $\sim 5 \times 10^5$ spectra. These spectra yield good line-of-sight velocities and estimates of $[\text{Fe}/\text{H}]$ errors of ~ 0.1 dex and a coarse estimate of $[\alpha/\text{Fe}]$. Three surveys (APOGEE, ESO-

Gaia and HERMES) are currently being prepared that will obtain large numbers of spectra with resolutions in the range 20 000 – 40 000 from which abundances of significant numbers of elements can be determined. Several important photometric surveys are currently under way, including the PanSTARRS survey (Kaiser et al. 2002) which is obtaining *griz* photometry through a large part of the sky, and surveys of the bulge region and the Galactic plane in the near-IR with the VISTA telescope. The era of great Galactic surveys will culminate in ESA’s Gaia mission, which is scheduled for launch in early 2013 and aims to return photometric and astrometric data for 10^9 stars and low-dispersion spectra for $\sim 10^8$ stars.

The Galaxy is an inherently complex object, and the task of interpreting observations is made yet more difficult by our location within it. Consequently, the ambitious goals that the community has set itself, of mapping the Galaxy’s dark-matter content and unravelling how the Galaxy was assembled, can probably only be attained by mapping observational data onto sophisticated models. This paper is the first in a series in which we use a new method of analysing dynamical models to interpret data from surveys of different types. Here we introduce and test the basic principles using mock survey catalogues of the region $b > 30^\circ$ that contain data of Gaia-like quality that progresses in completeness from photometry plus proper motions, through photometry, proper motions, parallaxes and line-of-sight velocities. In subsequent papers we will extend the formalism to include spectrophotometric data and apply it to real catalogues.

The paper is organised as follows. Section 2 explains the fundamental importance of equilibrium dynamical models

* E-mail: p.mcmillan1@physics.ox.ac.uk

for the problem in hand. Section 3 discusses the feasibility of using N-body models to interpret surveys of the Milky Way and outlines our preferred strategy. Section 4 presents the formulae used to calculate the likelihood of a catalogue given a model, while in Section 5 we explain how we find the optimum values of the model’s parameters and their statistical uncertainties. Section 6 describes how we construct a pseudo-catalogue from a model and a number of tests of our method that we have run using a Gaia-like pseudo-catalogue. Section 7 outlines a number of directions for further work and future developments of our methodology. Section 8 sums up.

2 WHY WE NEED GALAXY MODELS

Models of the Galaxy have a key role to play for several reasons. First they enable one to understand and compensate for observational biases, which dominate all data sets on account of our location in the Galaxy’s dust- and gas-rich disc. Second they provide the natural means of tying together data from different surveys – surveys may concentrate on obtaining photometric, astrometric or spectral data and different surveys probe magnitude ranges and therefore constrain the Galaxy over complementary distance ranges. A model can assemble this complementary information into a single coherent picture.

In the 1980s Bahcall and his collaborators moved Galactic astronomy an important step forward by introducing models of the stellar content of the Milky Way that were inspired by observations of external galaxies (Bahcall & Soneira 1984; Ratnatunga et al. 1989, and references therein). Although these models included the kinematics of stars, velocities were not required to be consistent with Newton’s laws of motion. In the Besançon model (Robin et al. 2003), Newton’s laws are used to connect the vertical structure of the disc to the distribution of vertical velocities, W , but the large-scale structure of the Besançon model of the Galaxy is not constrained by Newton’s laws. The most recent incarnation of this type of model is presented by Sharma et al. (2011).

Fully dynamical models, that is models in which the distribution of stars is consistent with Newton’s laws of motion, are now required for several reasons. Most obviously, the distribution of dark matter can be deduced from observations of stars and gas only by assuming that the Galaxy is in an approximate steady state, and interpreting observations in the framework of an *equilibrium* dynamical model – if we do not assume a steady state (which strictly speaking must be a false assumption), any mass distribution is consistent with any phase-space distribution of the baryonic matter. Inferences about the mass content can only be drawn because a sufficiently large central concentration of mass would imply a rapid collapse of the baryonic component from its observed configuration, and a sufficiently small mass concentration would imply that the baryonic component would fly apart. We must deduce the actual mass distribution by assuming that the baryonic component is in an approximate steady state, thus ruling out large-scale contraction or expansion. Hence equilibrium dynamical models are fundamental for achieving a major goal of contemporary astronomy.

An attractive feature of equilibrium dynamical models

is that they reduce the Galaxy from a six-dimensional to a three-dimensional object: without the assumption of dynamical equilibrium, we have to specify the distribution of stars in six-dimensional phase space, while the assumption of equilibrium together with Jeans’ theorem makes it sufficient to specify the distribution of stars in three-dimensional space of isolating integrals. For obvious reasons, objects can be imagined in three dimensions much more easily than they can be imagined in four or higher dimensions, so the reduction in dimensionality from six to three is a major simplification. This reduction also vastly reduces the amount of information required to specify a model: if we measure each position and velocity with a precision of, say, 1 percent, a six-dimensional model with less than 10^{12} resolution elements will degrade the resolution of the raw data, while a three-dimensional model requires only 10^6 resolution elements for a faithful representation of the data.

A dynamical model connects objects that we can observe to objects that we have not observed, either because they are distant and therefore faint, or because they are obscured by dust. For example May & Binney (1986) showed that if the stellar halo were in virial equilibrium, more than half the stars of the stellar halo would be on orbits that bring them through the solar neighbourhood, so in principle from measurements made in a small volume around the Sun we could determine the density of stars on more than half the halo’s populated orbits.

The Galaxy is certainly not in a steady state. Most obviously because it has a bar inside ~ 3 kpc and spiral arms in the surrounding disc. These features not only rotate with various pattern speeds, but on longer timescales change their structure and may well decay. Moreover, by scattering stars and dark-matter particles they drive secular evolution of all the Galaxy’s components. The resulting secular evolution of the disc has been studied for half a century (e.g. Roman 1954; Spitzer & Schwarzschild 1953; Carlberg & Sellwood 1985; Binney & Lacey 1988; Dehnen & Binney 1998; Schönrich & Binney 2009) and has clearly played a major role in determining the observed state of the Galaxy. Secular evolution is most readily modelled by adding perturbations to the Hamiltonian of an equilibrium model, that cause the model to move through a series of equilibrium states. Hence equilibrium models are the key to modelling secular evolution as well as to determining the distribution of dark matter.

Data from the SDSS survey revealed that a significant proportion of the stellar halo has yet to phase mix properly, and that it contains numerous tidal streams (Bell et al. 2008). These streams have considerable potential for mapping the Galaxy’s gravitational field and distribution of dark matter. Galaxy models of the type we advocate in this paper would seem to offer the best hope of fully exploiting the potential of tidal streams (Eyre & Binney 2011).

The complexity of the Galaxy is such that we cannot realistically hope eventually to build a dynamical model that accounts for *every* observation in detail. For example, it is known that stellar discs are highly responsive objects, and much of the Galaxy’s current spiral structure will represent an ephemeral response to noise driven by star formation and fluctuations in the density of the dark-matter halo. The Galaxy’s warp is likely to be driven by such density fluctuations. In these circumstances we should aim for a sequence of

dynamical models of increasing complexity and realism. We aim first for an axisymmetric, equilibrium model and identify the most prominent features in the data that cannot be explained by such a model. Then we aim for a steady-state barred model and see how much more of the data such a model can explain. Next we include either the warp or spiral structure by perturbing our best barred model, and see how much better we can fit the data. By proceeding in this way we can hope to reach the point at which we feel we have a model that provides as good a fit to the data as it is reasonable to expect, and we will have learnt along the way a great deal about the Galaxy’s contents and manner of operation. In this paper we are concerned with the first stage in this journey, the construction of axisymmetric models.

3 TYPES OF GALAXY MODEL

3.1 N-body models

The simplest galaxy models to construct are N-body models. The initial conditions from which an N-body model is integrated are generally not consistent with an equilibrium model because such initial conditions can only be chosen if one is already in possession of the desired model. Therefore the equations of motion must be integrated for some time to allow the model to settle to an equilibrium through relaxation. This period of relaxation has two unfortunate consequences. First, equilibrium is reached only asymptotically in time, and in the case of a disc galaxy significant relaxation may continue for an inconveniently long time. Second, it is not clear what initial conditions are required to achieve a given configuration. Recently the “made-to-measure” (M2M) technique introduced by Syer & Tremaine (1996) has been sharpened by de Lorenzi et al. (2007), Dehnen (2009) and others into an effective way to refashion a model that somewhat resembles the target galaxy into a model that represents that galaxy to good accuracy. Consequently the dynamical models that currently best approximate the Galaxy are M2M models (Bissantz et al. 2004; Martinez-Valpuesta & Gerhard 2011).

While M2M models can be extremely useful, they are less than ideal from a number of perspectives. First, an M2M model is specified by N phase-space coordinates and particle weights, where $N \gtrsim 10^5$ is a large number. This specification is at once cumbersome and non-unique; at a later time the coordinates will be different while the model will be the same. An equally good model of the same galaxy made by a different group will use a different mix of orbits so the weights will be different and it will not be evident that the two models are equivalent. Second, when the model’s phase space has significant stochastic regions, it is not possible to halt dynamical evolution of the model during the period that orbits are followed in order to optimise their weights. Finally, there is a fundamental problem with any particle-based model of the Galaxy that was pointed out by Brown et al (2005): important information about the Galaxy is contained in observations of low-luminosity stars that can only be observed close to the Sun, so such stars must be represented in any complete Galaxy model. However, orbiting particles that are at one moment near the Sun are some time later far from the Sun. If particles are treated as stars, those

that represent low-luminosity stars will rarely contribute to observables because the particle will usually be too far from the Sun to be visible. Consequently, the number of particles contributing to observables will be much smaller than the number of particles in the model. One might hope to circumvent this problem by considering particles to be representatives of a stellar population that has a well defined luminosity function. Then when a particle is far from the Sun, one could be sure to draw a representative star luminous enough to be visible from the Sun. But then for consistency *many* stars must be drawn from the particle when it is near the Sun. Clearly the model’s shot noise will be adversely affected if each nearby particle contributes to the observables a host of stars with exactly the same phase-space coordinates, just as it will be if the number of stars is much less than the number of particles.

To escape from this sampling problem we need to be able to sample the solar neighbourhood much more densely than far-flung parts of the Galaxy. That is, our model must yield the probability density of particles rather than a specific realisation of this density – we need to know the phase-space density f of stars, for armed with f we can populate the solar neighbourhood with large numbers of mostly low-luminosity stars and remote parts of the Galaxy with smaller numbers of exclusively luminous stars.

In principle it *is* possible to determine the phase-space density f from an N-body model because Liouville’s theorem assures us that phase-space density is constant along orbits, so the phase-space density is known at the location of every particle provided the initial conditions sampled a well defined sampling density f_s (e.g. §4.7.1 of Binney & Tremaine 2008). Hence the phase-space density at any point in the phase space of the final model can be estimated by six-dimensional interpolation. Sampling the phase-space density obtained in this way is not easy, but is achievable with the Metropolis algorithm for example (e.g. Binney et al. 1992, §4.3). However, these steps are highly non-trivial and to the best of our knowledge no N-body model has been successfully resampled.

The problem of determining the distribution function (DF) f is made more challenging by the fact that we need not one DF but a DF f_α for each stellar population α : as a minimum the model must predict the spatial distribution and kinematics of stars that lie in each of several regions of the $([\text{Fe}/\text{H}], [\alpha/\text{Fe}])$ plane (e.g. Schönrich & Binney 2009). It would not be straightforward to adapt an N-body model so that it yielded several DFs simultaneously, although *ab initio* models of galaxy formation can assign stellar parameters to particles (e.g. Simon et al. 2010, and references therein).

3.2 Torus models

The modelling technique introduced by Schwarzschild (1979) has become the standard tool for analysing the dynamics of early-type galaxies (e.g. Krajnović et al. 2005), especially in connection with searches for central black holes (e.g. Gebhardt et al. 2003). This technique involves first integrating a number of orbits in the adopted gravitational potential and then seeking weights for these orbits such that the weighted sum of the orbits reproduces the observational data to acceptable precision.

Torus modelling is analogous to Schwarzschild mod-

elling except that orbits, which are essentially time series of phase-space points, are replaced by orbital tori, which are analytic expressions for the three-dimensional continuum of phase-space points that are accessible to a star on a given orbit. Whereas an orbit is labelled by its initial conditions, a torus is labelled by its three action integrals J_i ; whereas position on an orbit is determined by the time t elapsed since the initial condition, position on a torus is determined by the values of three angle variables θ_i , one canonically conjugate to each action J_i . For a list of advantages arising from the replacement of orbits by tori, see Binney & McMillan (2011), and for a summary of how orbital tori are constructed and references to the papers in which torus dynamics was developed, see McMillan & Binney (2008). Note that torus models provide the ideal framework within which to study features such as spiral arms or warps because they come with angle-action variables; these coordinates were invented for perturbative studies of the solar system and, as Kaasalainen (1994) showed, perform spectacularly well when they have been derived by constructing tori.

Although it is possible to treat the weights of tori as independent unknowns to be fitted to the data just as in Schwarzschild modelling, a better procedure is to derive the weights from the model's DF. By Jeans' theorem, the DF of a steady-state model can be taken to be a function $f(\mathbf{J})$ of the action integrals. Following Binney (2010; hereafter B10) we make f an analytic function of certain parameters a_i in addition to \mathbf{J} , and we fit the model to the data by varying the a_i .

The impact of shot noise on the model is minimised if all tori have the same weight, and this will be the case if the density of used tori in action space samples the DF. We endeavour to ensure that this condition is met, at least to a good approximation.

4 ASSESSING A MODEL

Our modelling strategy is as follows. For each trial gravitational potential we construct a library of orbital tori that has a known sampling density in action space. For each of the Galaxy's identified stellar populations (such as G-dwarfs or K-giants of given metallicity) we have a luminosity function $F(M)$ and a trial DF with parameters that have to be chosen for that population. For given values of these parameters, we can infer the weight of each of the library's tori from the DF. Given these weights and the numerically-determined mapping from actions and angles to Cartesian phase-space variables, we can find the probability of finding a star of a given absolute magnitude at any point (\mathbf{x}, \mathbf{v}) in phase space, and therefore at any point in the space of observables. Hence for given values of the parameters we can evaluate the likelihood of the data given the model that is defined by the current gravitational potential and the current parameters. We find the values of the parameters that maximise the likelihood for the given potential, and then repeat the process for a different potential. In this way we determine what range of gravitational potentials and DFs is consistent with the data.

The Galaxy's gravitational potential Φ is generated by the sum of the mass densities of *all* the Galaxy's populations, including that of its dark-matter particles. Our knowl-

edge of Φ remains quite limited, so in the coming years the challenge is to use the kinematics of stars and gas to constrain Φ more tightly. Then Poisson's equation can be used to derive the dark-matter density as the difference between the density that generates Φ and the density of stars and gas. Once the distribution of dark matter is fairly well known, it will be appropriate to seek a DF for the dark matter and construct a completely self-consistent model of the Galaxy. At the present stage of our understanding a concern for self-consistency would be premature because many DFs for dark matter will be consistent with any plausible density distribution of dark matter. Consequently, nothing is to be gained by specifying the dark matter's DF until there are kinematic constraints on it, presumably provided by experiments that detect dark-matter particles underground.

In this paper our focus is on the determination of the DF of stars given typical observational data and a trial form for Φ . We defer to a subsequent paper a study of the effects of changing the assumed form of Φ and thus the extent to which given data allow one to constrain Φ .

4.1 Basic notation

We now lay out the formulae that are required to implement the strategy just described. The data consist of a catalogue that for N stars gives accurate values of the Galactic coordinates (b, l) , data such as apparent magnitude m , colour $V - I$, and line-of-sight velocity v_{los} that have moderate errors, and values of the parallax ϖ , proper motion $\boldsymbol{\mu}$, surface gravity g and metallicity Z that are probably significantly in error. We group the variables into two sets, the basic variables

$$\mathbf{u} \equiv (b, l, m, \varpi, \boldsymbol{\mu}, v_{\text{los}}) \quad (1)$$

and additional astrophysical variables

$$\mathbf{s} \equiv (V - I, g, Z). \quad (2)$$

Note that \mathbf{u} has seven components, effectively a star's phase-space coordinates (\mathbf{x}, \mathbf{v}) and its apparent magnitude m . For now we neglect interstellar extinction. Then the star's absolute magnitude M is effectively specified by \mathbf{u} because the star's distance is fixed by \mathbf{x} .

We assume that the errors in the observed quantities are independent and can be modelled by Gaussian probability distributions

$$G(u, \bar{u}, \sigma) \equiv \frac{e^{-(u-\bar{u})^2/2\sigma^2}}{\sqrt{2\pi\sigma^2}}. \quad (3)$$

We attach primes to the true values of measured quantities to distinguish them from the measured values, so we generically have that the probability of measuring a value u is

$$\text{Pr}_o(u) = \int du' G(u, u', \sigma) \text{Pr}_{\text{model}}(u'), \quad (4)$$

Any quantity such as the parallax that is not given in the catalogue can be considered to have a sufficiently large σ that the Gaussian density is effectively constant for all relevant values of the variable.

For brevity we use the notation

$$G_i^j(\mathbf{u}, \mathbf{u}', \boldsymbol{\sigma}) \equiv \prod_{k=i}^j G(u_k, u'_k, \sigma_k). \quad (5)$$

In this paper we restrict ourselves to the case of a single stellar population. This assumption ensures that there are no correlations between stellar type and kinematics: the distribution of stars in phase space is independent of their luminosities, colours, metallicities, etc. In this case we can confine discussion to the components of \mathbf{u} and neglect \mathbf{s} . We assume that the luminosity function $F(M)$ satisfies the normalisation condition

$$1 = \int_{-\infty}^{\infty} dM F(M) \quad (6)$$

and that the DF $f(\mathbf{J})$ is normalised such that

$$1 = \int_{\text{all } \mathbf{J}, \boldsymbol{\theta}} d^3\mathbf{J} d^3\boldsymbol{\theta} f(\mathbf{J}). \quad (7)$$

Note that $(\mathbf{J}, \boldsymbol{\theta})$ determines (\mathbf{x}, \mathbf{v}) , so the set $(M, \mathbf{J}, \boldsymbol{\theta})$ fixes the true values of a star's observables, \mathbf{u}' .

We require the probability of observing a star with observables in $d^7\mathbf{u}'$ given that the star satisfies the selection criteria of the survey. If $dP(\mathbf{u}')$ is the probability that a star chosen randomly from the Galaxy as a whole lies in $d^7\mathbf{u}'$ around \mathbf{u}' , then

$$dP(\mathbf{u}') = dP(\mathbf{u}'|\text{in survey})P(\text{in survey}). \quad (8)$$

But

$$dP(\mathbf{u}') = f(\mathbf{J})F(M) \frac{\partial(M, \mathbf{J}, \boldsymbol{\theta})}{\partial(\mathbf{u}')} d^7\mathbf{u}', \quad (9)$$

so

$$P(\mathbf{u}'|\text{in survey}) d^7\mathbf{u}' = \frac{f(\mathbf{J})F(M)}{P(\text{in survey})} \frac{\partial(M, \mathbf{J}, \boldsymbol{\theta})}{\partial(\mathbf{u}')} d^7\mathbf{u}'. \quad (10)$$

To take into account observational errors, we fold the probability distribution (10) with the Gaussian kernel and have that the probability density of stars in the space of observables that is predicted by the DF f is

$$\begin{aligned} \text{Pr}_o(\mathbf{u}|f) &= \int d^7\mathbf{u}' G_1^7(\mathbf{u}, \mathbf{u}', \boldsymbol{\sigma}) P(\mathbf{u}'|\text{in survey}) \\ &= \frac{\int d^3\mathbf{J} f(\mathbf{J}) \int d^3\boldsymbol{\theta} \int dM F(M) G(\mathbf{u}, \mathbf{u}', \boldsymbol{\sigma})}{P(\text{in survey})}, \end{aligned} \quad (11)$$

where $\mathbf{u}'(M, \mathbf{J}, \boldsymbol{\theta})$ is the vector of observables corresponding to the given absolute magnitude and phase-space position.

Since $\text{Pr}_o(\mathbf{u}|f)$ is a properly normalised probability density function (pdf), we have

$$\begin{aligned} P(\text{in survey}) &= \int d^3\mathbf{J} f(\mathbf{J}) \int d^3\boldsymbol{\theta} \int dM F(M) \\ &\quad \times \int_S d^7\mathbf{u} G(\mathbf{u}, \mathbf{u}', \boldsymbol{\sigma}) \end{aligned} \quad (12)$$

where the subscript S on the second integral implies integration through the range of observables encompassed by the survey. Usually, there is no restriction on the velocities, so the Gaussian factors in μ_b , etc, integrate out to unity. Similarly the parallax will not be restricted a priori, so its Gaussian factor will integrate to unity. We assume that the Gaussian factors in b and l integrate to either zero or unity, depending on whether the true values b' and l' lie in the surveyed region because the observational errors in the sky coordinates are so small. Hence only the integral over apparent magnitude m need be considered, and in this paper we make the assumption that the errors in m are small

compared to the width of the luminosity function, so we assume that the remaining integral is zero or unity depending on whether the true apparent magnitude m' lies within the survey limits. Thus we adopt

$$P(\text{in survey}) = \int d^3\mathbf{J} f(\mathbf{J}) \int_S d^3\boldsymbol{\theta} \int_{-\infty}^{M_{\text{crit}}(r)} dM F(M), \quad (13)$$

where $r(\mathbf{J}, \boldsymbol{\theta})$ is the heliocentric distance of the specified point in phase space and

$$M_{\text{crit}}(r) = m_{\text{lim}} - 5 \log_{10}(r/10 \text{ pc}) \quad (14)$$

with m_{lim} the limiting apparent magnitude of the survey. We define the survey's selection function to be

$$\phi(\mathbf{J}) = \int_S d^3\boldsymbol{\theta} \int_{-\infty}^{M_{\text{crit}}(r)} dM F(M), \quad (15)$$

Then we have

$$P(\text{in survey}) = \int d^3\mathbf{J} f(\mathbf{J}) \phi(\mathbf{J}), \quad (16)$$

and (11) can be written

$$\text{Pr}_o(\mathbf{u}|f) = \frac{\int d^3\mathbf{J} f(\mathbf{J}) \int_S d^3\boldsymbol{\theta} \int dM F(M) G(\mathbf{u}, \mathbf{u}', \boldsymbol{\sigma})}{\int d^3\mathbf{J} f(\mathbf{J}) \phi(\mathbf{J})}. \quad (17)$$

From these individual probabilities we construct the log likelihood of a survey for a given model:

$$L \equiv \sum_{\alpha} \ln [\text{Pr}_o(\mathbf{u}_{\alpha}|f)], \quad (18)$$

where the sum is over the stars in the survey. In an appendix we demonstrate explicitly that L is stationary when the trial DF used to evaluate it is equal to the DF that was used to produce the catalogue being analysed.

The integrals over \mathbf{J} in equation (17) are most conveniently done by Monte-Carlo integration. We arrange that the points at which the integrand is evaluated sample the DF, so we may replace $\int d^3\mathbf{J} f(\mathbf{J})$ by $N^{-1} \sum_k$:

$$\text{Pr}_o(\mathbf{u}|f) = \frac{\sum_{k=1}^N \int_S d^3\boldsymbol{\theta} \int dM F(M) G_1^7(\mathbf{u}, \mathbf{u}'_k, \boldsymbol{\sigma})}{\sum_k \phi(\mathbf{J}_k)} \quad (19)$$

where $\mathbf{u}'_k(M, \mathbf{J}_k, \boldsymbol{\theta})$.

The evaluation of the integral in equation (19) can be simplified by taking advantage of the fact that the errors in (b, l) are small so the integrand is non-negligible only when (b', l') lies close to (b, l) . We can approximate the Gaussians in these variables as δ -functions and integrate them out analytically: doing so we introduce a Jacobian because

$$\begin{aligned} &\int d^3\boldsymbol{\theta} \delta(b - b') \delta(l - l') \\ &= \int db' dl' d\varpi' \left| \frac{\partial(\boldsymbol{\theta})}{\partial(b', l', \varpi')} \right| \delta(b - b') \delta(l - l') \\ &= \int d\varpi' \left| \frac{\partial(\boldsymbol{\theta})}{\partial(b, l, \varpi')} \right|. \end{aligned} \quad (20)$$

The evaluation of the Jacobian is described in the Appendix of Binney & McMillan (2011). Now we have

$$\text{Pr}_o(\mathbf{u}|f) = \frac{\sum_k \int dr' \left| \frac{\partial(\boldsymbol{\theta})}{\partial(b, l, r')} \right| \int dM F(M) G_3^7(\mathbf{u}, \mathbf{u}'_k, \boldsymbol{\sigma})}{\sum_k \phi(\mathbf{J}_k)}, \quad (21)$$

where the integration over the true parallax $\varpi' = 1/r'$ has been transformed into an integration over true heliocentric distance. The integral over M simply returns the fraction of the stellar population that is consistent with the measured apparent magnitude at distance r' . We use equation (21) for $\text{Pr}_o(\mathbf{u}|f)$ in equation (18) when evaluating the likelihood.

We determine $\phi(\mathbf{J})$ as follows. For each value of \mathbf{J} we choose at random a point θ_i in angle space. The point corresponds to a distance r and sky coordinates (b, l) . If these coordinates lie in the survey volume, stars with brighter absolute magnitudes than the value $M_{\text{crit}}(r)$ from equation (14) will enter the catalogue. After a large number N of values of θ have been explored, we have

$$\phi(\mathbf{J}) \simeq \frac{1}{N} \sum_{i=0}^N \int_{-\infty}^{M_{\text{crit}}(r_i)} dM F(M). \quad (22)$$

Since ϕ does not depend on f , it needs to be evaluated only at the start of the procedure for optimising f .

The survey contains no information about the value of $f(\mathbf{J})$ at actions for which $\phi(\mathbf{J}) = 0$, so it is immaterial whether we change the value of f at these actions. When we adopt a functional form for f , we are in fact varying f in these invisible regions, and thus at the end of the process arrive at a prediction for that can be tested by a deeper or wider survey.

4.2 Binning the data

The computational cost of evaluating the likelihood of a catalogue scales as the product of the number of stars in the catalogue and the number of tori used to sample the model. Even for a catalogue that contains $\sim 10^5$ stars, the cost is high. We now investigate the scope for reducing the cost by binning the data.

The log likelihood (18) is a sum of the contributions from individual stars. Since the contribution from an individual star is practically unchanged by shifting its point \mathbf{u} in data space by a small amount within the core of its error ellipsoid, the calculated likelihood of the catalogue will not change much if we group stars with data points that lie within a small cell in data space and attribute to all of them the contribution to L from the centre of the bin. A slightly refined version of this basic idea is as follows.

We establish a Cartesian grid in data space, the cell spacing in most dimensions being of order half the typical observational uncertainty of the corresponding observable. If we applied this criterion to l and b , we would obtain an absurdly fine grid on the sky. Therefore, in l and b we take the separation between bins to be comparable to the changes in angle over which we expect the distribution of stars to change significantly – this might be as large as 10° in l and a degree or so in b at low latitudes and larger increments near the poles. Having established our grid, we assign stars to cells. Finally we evaluate Pr_o at the centre of each cell and form L by adding the logarithm of this value times the number of stars assigned to that cell. The saving in computation from binning is clearly proportional to the number of stars assigned to each cell, which increases with the adopted bin sizes and decreases with the number of quantities actually observed. Hence binning is most attractive for the sparsest data set, namely measurements of (b, l, m, μ) . However, this

is already a five-dimensional space. For a survey of a third of the sky, it might be possible to get by with 100 bins on the sky. A few tens of bins would be required for the apparent magnitudes, and for each component of μ ten bins might suffice. Thus a minimal grid will have $> 10^5$ bins, so even with the simplest conceivable data, binning first becomes advantageous when the number of stars in the catalogue exceeds a million. In the case of Gaia, the list of observables must be expanded to include at least ϖ , and the number of bins required to do justice to the proper-motion data must be increased by a factor of at least 10, implying a grid with $> 10^6$ bins. In reality one would want to include colour data, and some line-of-sight velocities, and the number of bins would be pushed up to $\sim 10^9$, essentially the number of stars in the catalogue.

Thus on account of the high dimensionality of the problem posed by current and future surveys of the Galaxy, the prospects for binning reducing the computational cost of fitting models are not bright.

5 OPTIMISING THE DF

The formulae of the last section are used to evaluate the log likelihood L of a catalogue given a particular model. In this section we explain how we estimate the probability distributions of the parameters that appear in the DF. We do this with the Markov Chain Monte-Carlo (MCMC) algorithm: we choose some plausible set of parameters \mathbf{a} for the DF and evaluate L for these parameters. Then we generate a random change $\delta\mathbf{a}$ in the parameters and evaluate L for the DF with parameters $\mathbf{a}' \equiv \mathbf{a} + \delta\mathbf{a}$. If the new value L' exceeds the old value L , we set $\mathbf{a} = \mathbf{a}'$, while if $L' < L$ we set $\mathbf{a} = \mathbf{a}'$ with probability $\exp(L' - L)$. After a sufficient time, the resulting sequence of values of \mathbf{a} sample the underlying PDF of \mathbf{a} (e.g. §4.3 of Binney et al. 1992).

Thus our approach to model fitting employs Monte-Carlo sampling in two distinct ways. To evaluate L for any given parameters \mathbf{a} we evaluate the action-space integral by Monte-Carlo sampling action space, and to determine the PDF of the parameters of f we Monte-Carlo sample parameter space.

It is useful to keep a record of the individual contributions to the sums over k in equation (21) for the following reason. Once the likelihood of the data given the current DF f has been evaluated, a neighbouring DF, \tilde{f} , is chosen, and the likelihood is re-evaluated. The new value of any sum over k can be obtained by, in equation (21), making the replacement

$$\sum_k \rightarrow \sum_k [\tilde{f}(\mathbf{J}_k)/f(\mathbf{J}_k)]. \quad (23)$$

Consequently, if when we first evaluate the likelihood of the catalogue we record for each star the contribution that each torus makes to the probability of seeing that star, we can evaluate the likelihood of the catalogue for any other DF at speed. The price of this speed is having to record an array of size the number of stars in the catalogue times the number of tori employed. Fortunately, the array is somewhat sparse because a significant fraction of tori make a negligible contribution to the likelihood of a given star. The more precise the data are, the sparser the array becomes.

A key to computational efficiency on the first evaluation of the likelihood of the catalogue is to identify in advance for each star the limited number of tori that contribute significantly to the integral in equation (21). To do so efficiently we create, for each torus, a grid in l, b and heliocentric r , and store the ranges of possible v_l, v_b and v_{los} for each bin in the grid that the torus goes through (found to a good approximation by sampling at many θ from the torus). With this information we can then, for each star, quickly discard tori which are clearly not relevant because the bins associated with the appropriate line of sight are either empty or have r and/or velocity ranges which are clearly incompatible with the observations.

For a catalogue of significant size the extra computational effort required to produce these grids is small compared to the computational effort saved by reducing the number of integrals that need to be performed because a grid only needs to be computed once per torus, rather than once per star per torus. In the examples discussed in Section 6 the grids reduce the number of line-of-sight integrals which need to be found by between a factor of ~ 10 when only μ is provided, and a factor of ~ 50 when μ, v_{los} and ϖ are provided.

5.1 How many tori do we need?

As just explained, estimates of L for many different parameter values are obtained with the same set of representative tori, and the final optimum values of the parameter and their uncertainties are usually based on a single set of sampling tori. Unless this set is sufficiently rich, the parameter estimates are likely to be biased in the sense that their optimum values differ from the true values by more than the returned uncertainties: the latter reflect both the input observational errors and the statistical uncertainty arising from the finite number of stars in the catalogue we are fitting. They do not include statistical error associated with the use of a finite number of tori to evaluate integrals over action space.

So, how many tori do we need to use? It is evident that at least one torus must yield a point \mathbf{u}' in the space of observables that lies within $\sim 1\sigma$ of the measured location of each star. Stars for which only one torus contributes points to the 1σ error ellipsoid tend to bias the parameter values: in order to make such stars probable the computer has to make that torus probable; if this torus differs significantly from the star's actual torus, the probability associated with that star is being misplaced within action space, and we infer an incorrect DF. For safety we require several tori to contribute points to the 1σ error ellipsoid, for then the greatest weight can be assigned to whichever one of them lies close to the star's true torus. Clearly the higher the quality of the catalogue, the smaller are the error ellipsoids and the more tori are needed to fulfil the criterion that several tori contribute to every 1σ error ellipsoid.

We can quantify this idea as follows. Equation (21) gives the probability of finding a star with observables \mathbf{u} as a sum of contributions from individual tori. If we define

$$p_k \equiv \frac{\int dr' \left| \frac{\partial(\theta)}{\partial(b, l, r')} \right| \int dM F(M) G_3^7(\mathbf{u}, \mathbf{u}'_k, \boldsymbol{\sigma})}{\text{Pr}_o(\mathbf{u}|f) \sum_{k'} \phi(\mathbf{J}_{k'})}, \quad (24)$$

then we have $\sum_k p_k = 1$ and the contribution of the k th

torus to $\text{Pr}_o(\mathbf{u}|f)$ is proportional to p_k . The Shannon entropy of the probability distribution $\{p_k\}$,

$$S(\mathbf{u}|f) = - \sum_k^N p_k \ln p_k, \quad (25)$$

is the natural measure of the extent to which the probability $\text{Pr}_o(\mathbf{u}|f)$ is contributed by a large number of terms in the sum or dominated by a single largest contribution: S vanishes if there is one dominant contribution, so $p_k = \delta_{kk_0}$, and peaks at $S = \ln N$ when $p_k = 1/N$ for all k ; if there are just $n \ll N$ tori that might plausibly produce the data for a given star, n of the p_k will be of order $1/n$ and the rest will vanish, so the entropy will be of order $S \simeq \ln n$. Hence e^S is quite generally an estimate of the number of tori that are consistent with the star's data. Using too few tori to conduct the sum in equation (21) is signalled by some stars having values of e^S smaller than unity/a few and results in the formal errors on the parameters being too small, with the result that the true parameters lie outside the $\sim 1.5\sigma$ error ellipsoid.

While having $e^S \sim 1$ suggests that too few tori are being used, the following argument shows that a larger value of e^S does not guarantee that enough tori are being used to give reliable results. Two small samples of tori drawn from different DFs can by chance have almost identical distributions in action space. Suppose this distribution happens to fit the data perfectly. Then the two different parent DFs will appear to maximise the likelihood of the data, depending on which DF the tori were in fact drawn from. The best way to check that enough tori are being used is to draw a new sample of tori from the DF that maximises the likelihood with the original sample of tori, and then to repeat the maximisation process using the new tori in the analysis. If enough tori were used, the new pdf of the DF will differ negligibly from the old one.

6 TESTS

In this section we test the ability of our procedure to recover from a mock catalogue the DF from which the catalogue was obtained. Hence we (i) build a dynamical model with known DF, (ii) draw a sample of pseudodata from this model by “observing” it from the location of the Sun and then add errors to the “observations”, and (iii) use the algorithm described in Section 5 to constrain the DF. In this final step we assume the correct functional form for the DF and enquire how accurately we can recover from the pseudodata the values of the DF's parameters. We take the distance from the Galactic Centre to the Sun to be $R_0 = 8.5 \text{ kpc}$.

6.1 The adopted luminosity function

Since the velocity we infer for a star from its proper motion is proportional to the star's distance, whatever distance information we have is going to be crucial for the model-fitting process. For simplicity, we are assuming that the Galaxy contains a single stellar population, and we are not using colour information. Consequently, it suffices to specify the luminosity function. We use a simple polynomial approxi-

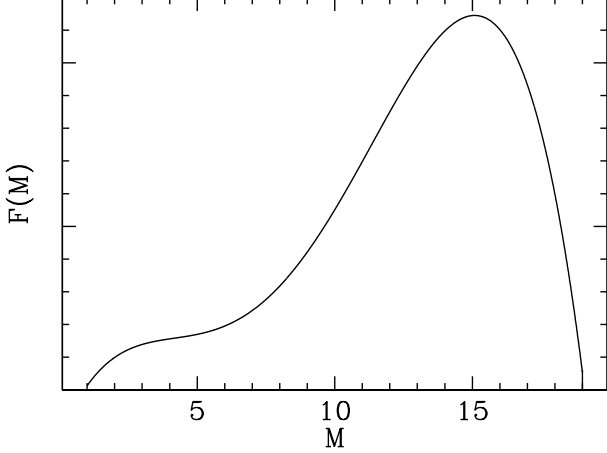


Figure 1. Luminosity function described in Section 6.1, and used in all tests.

mation to the general V -band luminosity function described in Binney & Merrifield (1998) Table 3.16:

$$F(M) \propto \begin{cases} -14.9 + 21M - 5.4M^2 \\ \quad + 0.59M^3 - 0.019M^4 & \text{for } 1 < M < 19 \\ 0 & \text{otherwise.} \end{cases} \quad (26)$$

This function is plotted in Figure 1.

6.2 The adopted gravitational potential

We use the Galactic potential which McMillan (2011) gives for a “convenient” Galaxy model. This axisymmetric model consists of a Galactic bulge, thin and thick exponential discs, and a Navarro, Frenk & White (1996) halo. The potential defines the Local Standard of Rest (LSR) and we assume that the Sun’s velocity with respect to the LSR is that given by Schönrich, Binney & Dehnen (2010).

6.3 The adopted distribution function

We have run tests using two model Galaxies, both based on a “quasi-isothermal” DF (Binney & McMillan 2011)

$$f(J_r, L_z, J_z) = f_{\sigma_r}(J_r, L_z) \times \frac{\nu_z}{2\pi\sigma_z^2} e^{-\nu_z J_z / \sigma_z^2}, \quad (27)$$

where

$$f_{\sigma_r}(J_r, L_z) \equiv \frac{\Omega\Sigma}{\pi\sigma_r^2\kappa} \bigg|_{R_c} [1 + \tanh(L_z/L_0)] e^{-\kappa J_r / \sigma_r^2}. \quad (28)$$

Here $\Omega(L_z)$ is the circular frequency for angular momentum L_z , $\kappa(L_z)$ is the radial epicycle frequency and $\nu(L_z)$ is its vertical counterpart. $\Sigma(L_z) = \Sigma_0 e^{-(R-R_c)/R_d}$ is the (approximate) radial surface-density profile and we set $R_d = 3$ kpc, where $R_c(L_z)$ is the radius of the circular orbit with angular momentum L_z . The factor $1 + \tanh(L_z/L_0)$ in equation (28) is there to effectively eliminate stars on counter-rotating orbits; the value of L_0 is unimportant in this study provided it is small compared to the angular momentum of the Sun. In equations (27) and (28) the functions $\sigma_z(L_z)$ and $\sigma_r(L_z)$ control the vertical and radial velocity dispersions. The observed insensitivity to radius of the scale-heights of

Table 1. The parameters of the DF of the model that contains both thin and thick discs

Disc	R_d/kpc	$\sigma_{r0}/\text{km s}^{-1}$	$\sigma_{z0}/\text{km s}^{-1}$	$L_0/\text{kpc km s}^{-1}$
Thin	3.0	27	20	10
Thick	3.5	48	44	10

extragalactic discs motivates the choices

$$\begin{aligned} \sigma_r(L_z) &= \sigma_{r0} e^{q(R_0 - R_c)/R_d} \\ \sigma_z(L_z) &= \sigma_{z0} e^{q(R_0 - R_c)/R_d}, \end{aligned} \quad (29)$$

where $q = 0.45$ and σ_{r0} and σ_{z0} are approximately equal to the radial and vertical velocity dispersions at the Sun. For discussion of the value of q and these choices of functional form, see B10.

The first distribution function we consider is a single thin quasi-isothermal disc, which was constructed with $R_d = 3$ kpc, $L_0 = 10$ kpc km s^{−1} and $\sigma_{r0} = \sigma_{z0} = 10$ km s^{−1}. This is rather dynamically cold, but we use it as a simple example to demonstrate and test the basic principles of the apparatus.

We have also tested the apparatus on a more realistic model Galaxy that has both thin and thick discs, with the thick disc contributing 23 per cent of the total disc surface density at the Sun. Table 1 gives the values of the parameters in the DF of this model.

B10 showed that by superposing a large number of DFs of a very similar form to these quasi-isothermal DFs, one can obtain a model that is consistent with the local stellar density and velocity distribution. In this study we, like Binney & McMillan (2011), restrict ourselves to these simple one- or two-disc models in order to provide some straightforward demonstrations of the principles discussed in Section 4. Extending this work to the more complicated DFs used by B10 is in principle straightforward.

6.4 Constructing a pseudo-catalogue

To construct a pseudo-catalogue of stars, we first randomly sample the distribution function in action space. If we take care to choose f so it can be evaluated without actually constructing a torus (which requires that it does not contain exact orbital frequencies) very little work is involved in evaluating $f(\mathbf{J})$ so MCMC sampling, in which at best a third of the points investigated are actually selected, is not expensive. For each chosen \mathbf{J} a torus is constructed.

Our tests are performed with a pseudo-catalogue that is magnitude limited with maximum apparent magnitude $m = 17$, and we confine the pseudo-catalogue to $b > 30^\circ$ because we have neglected extinction. The shape of the survey volume is then comparable to that of recent surveys (e.g. SDSS, RAVE). For each computed torus we evaluate the selection function $\phi(\mathbf{J})$ as described in Section 4.1. For some of our selected values of \mathbf{J} , the selection function will vanish because the torus does not intersect the survey volume. Such tori may be excluded from the list and it is in fact convenient to identify many of these tori in advance of computing them. Specifically, for a reasonable number of points in the J_r, J_ϕ plane we find the minimum value of J_z that takes a torus with given J_r and J_ϕ into the survey volume – this is conveniently done using the adiabatic approximation (Bin-

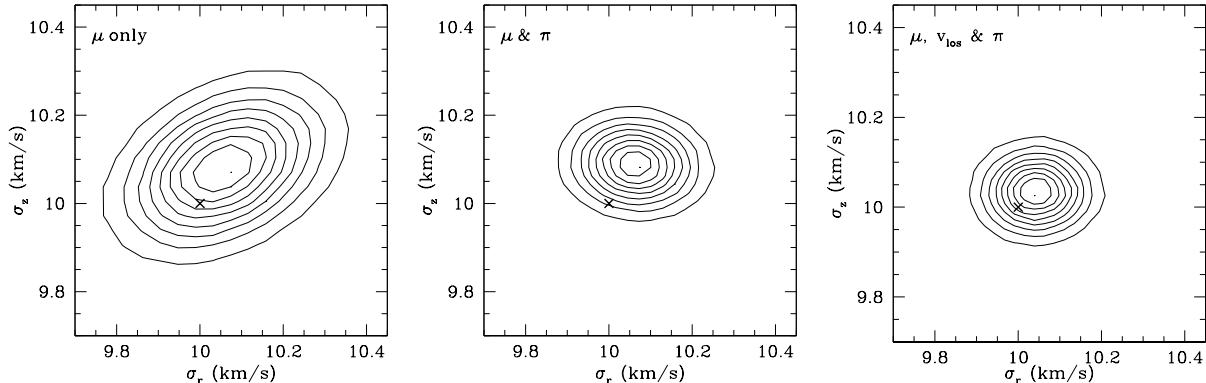


Figure 2. Tests of our ability to recover the parameters of the DF a catalogue of 5000 stars. Each panel shows the pdf of the DF in the $(\sigma_{r0}, \sigma_{z0})$ plane. The data from which these pdfs were recovered included photometry and proper motions in all three cases. The extreme left panel gives the pdf when no additional data are available, the centre panel shows what is achieved by adding parallaxes, and the rightmost panel shows the pdf when both parallaxes and line-of-sight velocities are available. Contour levels are at $n/9$ of the peak probability density, where $n = 1, \dots, 8$. The cross marks the true value of the parameters.

Table 2. Means and dispersions in km s^{-1} of parameters of the DF recovered from data made with just a thin disc. The first three columns give results for a catalogue with 5000 stars in a catalogue with Gaia-like measurement errors. The last two columns give the uncertainties arising from finite catalogue size with 5000 and 10000 stars in an error-free catalogue.

	μ only	Gaia-like errors		perfect data	
		μ, ϖ	$\mu, \varpi, v_{\text{los}}$	5000 stars	10000 stars
σ_{r0}	10.06 ± 0.14	10.06 ± 0.09	10.044 ± 0.075	10.02 ± 0.07	10.06 ± 0.05
σ_{z0}	10.08 ± 0.10	10.09 ± 0.06	10.03 ± 0.06	9.97 ± 0.05	9.97 ± 0.04

ney & McMillan 2011; Schönrich & Binney 2011). Then by interpolating between these values we can assess whether a given point \mathbf{J} is well outside the region of action space that can contribute to the catalogue.

To add a star to the catalogue, we select a torus from our list at random. Then we choose a value for each θ_i at random between 0 and 2π , and an absolute magnitude M randomly from our luminosity function (eq. 26). This defines the position, velocity, and apparent magnitude of a star. Observational errors are then added to the observational data for each star. The assumed errors were 0.2 mas in parallax, 0.2 mas yr^{-1} in proper motion, and 5 km s^{-1} in line-of-sight velocity. The star enters the catalogue if its observational data place it within our survey limits, and is discarded otherwise. We repeat this process until we have produced a catalogue of the desired size.

6.5 Case of only a thin disc

Fig. 2 shows the pdfs of the parameters σ_{r0} and σ_{z0} for the pure thin-disc model when there are data for 5000 stars and only photometry and proper motions are available (leftmost panel), or parallaxes are also available (central panel), or both parallaxes and line-of-sight velocities are available (rightmost panel). The means and dispersions of these pdfs are given by the last three columns of Table 2. We see that in all three cases, the true parameter values lie within the expected error ellipse and the uncertainties of the parameters are < 1.5 per cent. We obtained these results using 40000 tori with non-vanishing values of $\phi(\mathbf{J})$.

The situation when neither parallaxes nor line-of-sight velocities are available is of particular interest. Given the

breadth of the luminosity function plotted in Fig. 1, it is remarkable that the parameters can be determined with such precision because to do this, the algorithm has to correctly infer the typical velocities of stars, and it can deduce a velocity from a given proper motions only by correctly inferring the distance. By itself the broad luminosity function does not provide sufficient distance information. The required distance information is inferred by piecing together several lines of evidence. For example, in the given potential, a model with larger values of σ_{r0} and σ_{z0} would have a thicker disc, so stars seen at $b = 30^\circ$ along $l = 0$ and $l = 180^\circ$ would typically have Galactocentric radii that differed more than in a model with small σ_{i0} . Consequently, the ratio of the stellar densities seen along $l = 0$ and $l = 180^\circ$ increases with the σ_{i0} , and from the ratio present in the data the algorithm can constrain the σ_{i0} . An independent constraint is provided by the Sun's motion with respect to the LSR, since both the asymmetric drift of the disc and the typical distance to stars vary with the σ_{i0} , so the dispersions are constrained by the mean proper motion of disc stars. This is essentially the classical concept of secular parallax (e.g. §2.2.3 of Binney & Merrifield 1998) in a sophisticated context.

When only proper motions are available, the error ellipse is tilted with respect to the axes in the sense of a positive correlation between σ_{r0} and σ_{z0} . The correlation arises because increasing σ_{z0} without increasing σ_{r0} would, for example, at $l \simeq 90^\circ$ increase μ_b without increasing μ_l , and this would be apparent in the data. The impact on the data of increasing both dispersions in step can be to some extent masked by increasing the assumed distances to stars. The central panel of Fig. 2 shows that adding parallaxes eliminates this correlation. The panel on the extreme right of

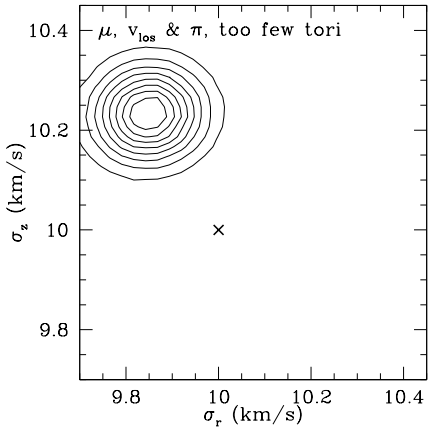


Figure 3. A bias introduced by using too few tori. Here only 2000 tori have been used to recover the parameters of the DF of the single-disc model.

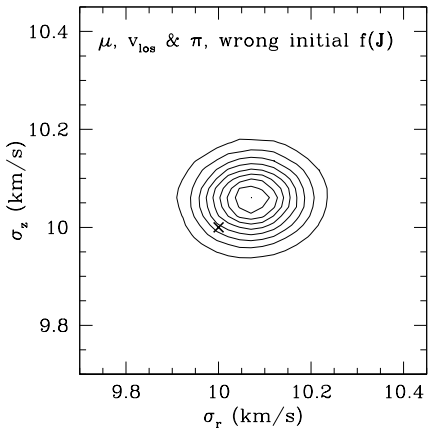


Figure 4. The pdf in the $(\sigma_{r0}, \sigma_{z0})$ plane for the same catalogue as that used in rightmost panel of Fig. 2, when an incorrect trial DF (with $\sigma_{r0} = \sigma_{z0} = 12 \text{ km s}^{-1}$) was used to perform the original integral over \mathbf{J} .

Fig. 2 shows that for this model little is gained by adding line-of-sight velocities with errors of 5 km s^{-1} , presumably because the random motions of the stars are so small.

6.5.1 Case of too few tori

In Section 5 we noted that using too few tori is liable to produce biased results. This phenomenon is illustrated by Fig. 3, which shows the same results as the rightmost panel of Fig. 2 except that 2000 rather than 40000 tori have been used in the analysis. The algorithm deduces that $\sigma_{r0} = (9.85 \pm 0.07) \text{ km s}^{-1}$, $\sigma_{z0} = (10.23 \pm 0.06) \text{ km s}^{-1}$ so the central values lie over 3σ from the truth.

6.5.2 Choice of trial distribution function

The Monte-Carlo integrals over \mathbf{J} in equation (17) are performed using an initial trial DF, which then allows us to evaluate the likelihood of similar DFs using the substitution given in equation (23). In the other cases reported in this

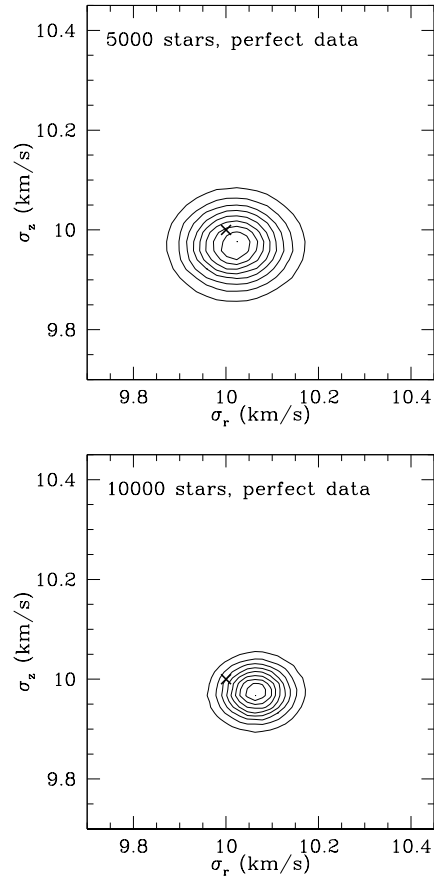


Figure 5. The pdf in the $(\sigma_{r0}, \sigma_{z0})$ plane when the only source of uncertainty is the finite size of the catalogue.

study we use the DF from which the stars were drawn as this trial DF, for convenience. To use this method in practice we need to be confident that it returns a correct result when a different trial DF is used.

In Fig. 4 we show the pdf in the $(\sigma_{r0}, \sigma_{z0})$ plane found for the thin-disc DF using the same input catalogue as that used to produce the rightmost panel of Fig. 2 and the rightmost column of Table 2, but with an initial trial DF which is a “quasi-isothermal” disc with $\sigma_{r0} = \sigma_{z0} = 12 \text{ km s}^{-1}$. The algorithm finds the results $\sigma_{r0} = (10.07 \pm 0.08) \text{ km s}^{-1}$, $\sigma_{z0} = (10.06 \pm 0.06) \text{ km s}^{-1}$, which is very close to the result found with the correct trial DF. Using a trial DF which differs from the true DF does reduce the effective number of tori which are used to determine the true DF, as it places an excessive number of tori in some regions of limited interest in action space, leaving a reduced number of tori in the relevant regions in action space. If the DF determined by the algorithm differs significantly from the trial DF it is sensible to use the DF that is determined as a new initial trial DF, and repeat the analysis to ensure that the results are not biased by the low effective number of tori.

6.5.3 Irreducible statistical error

Even with error-free data it cannot be possible to constrain the parameters in the DF tightly if the catalogue is small. To determine the size of the uncertainty that is inherent in

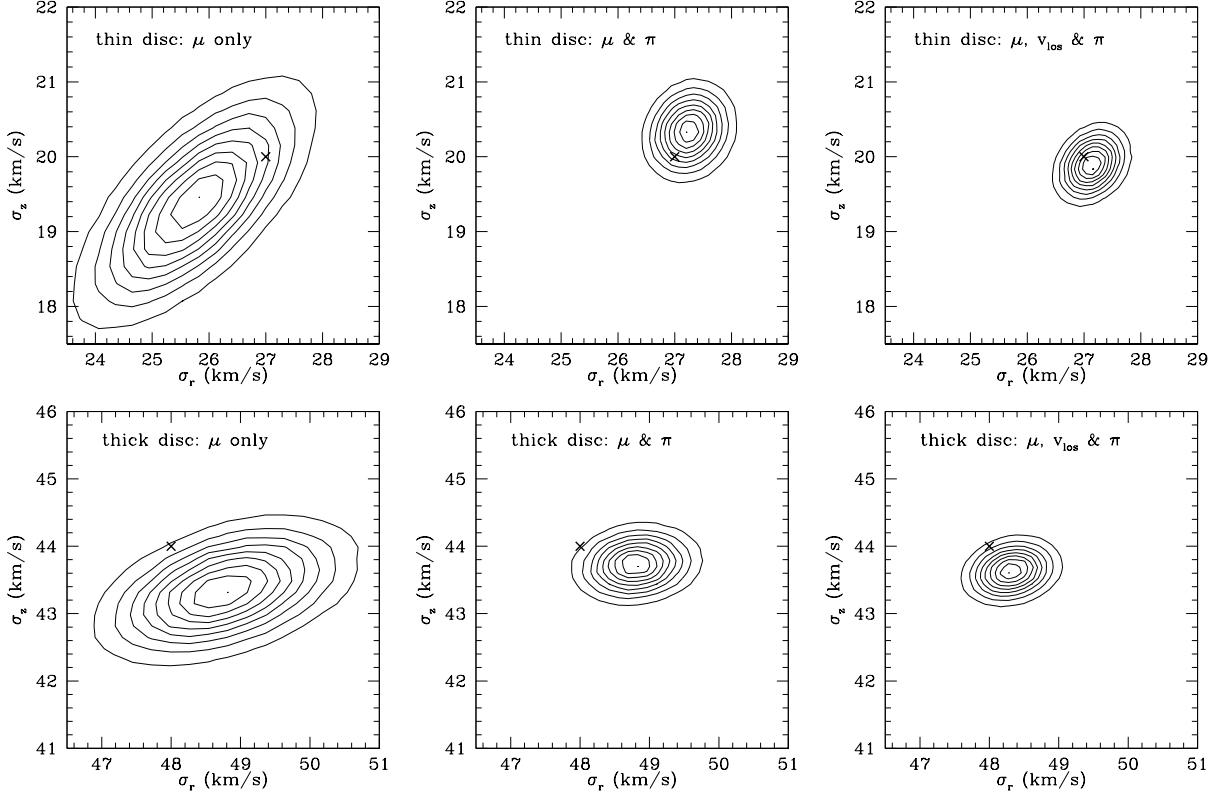


Figure 6. As Fig. 2 but for the case of both thin and thick discs and using a catalogue with 10 000 stars. The top row shows the pdfs for the parameters of the thin disc after marginalisation over the parameters of the thick disc, while the bottom row shows those for the thick disc, similarly marginalised.

using only a finite number of stars we must do two things: (i) consider a catalogue with error-free data, and (ii) analyse this catalogue using precisely the tori that were used to generate the catalogue. This second step eliminates any bias arising from the use of a finite number of tori to evaluate the integral over \mathbf{J} by Monte-Carlo integration by the following argument. With error-free data, only the star's true torus will assign a non-zero probability to the star, so it is important to be sure that this torus is present. Given that it is present, the Monte-Carlo estimate of the integral over \mathbf{J} will be exact, so the only source of uncertainty in the parameters of the DF will be the finite size of the catalogue.

Fig. 5 shows the results of running this test on the single-disc model when we have perfect measurements of proper motion, parallax and v_{los} for 5 000 stars (top) or 10 000 stars (bottom). The means and dispersions of the parameters in each case are given in the first two columns of Table 2. By resampling the DF to obtain different discrete realisations, one can directly verify that the formal errors shown in Table 2 are a fair indication of the uncertainty in the DF that is inherent in the size of the stellar sample. The decrease in the uncertainty of both σ_{r0} and σ_{z0} with increasing number N of stars in the catalogue is consistent with $\sigma_{i0} \propto 1/\sqrt{N}$. With 5 000 stars the irreducible statistical uncertainty is ~ 50 percent of the uncertainty with Gaia-like errors in the proper motions, even with no further information. The addition of the parallax to the data set reduces the uncertainty with Gaia-like errors to very little more than the uncertainty with perfect data.

Table 3. Means and dispersions in km s^{-1} of the parameters of the DF recovered from data made with a Galaxy that has both thin and thick discs, the analysed catalogue containing 10 000 stars

	μ only	μ, ϖ	$\mu, \varpi, v_{\text{los}}$
σ_{r0}	25.7 ± 0.99	27.2 ± 0.39	27.1 ± 0.33
σ_{z0}	19.4 ± 0.78	20.3 ± 0.32	19.9 ± 0.26
σ_{r0}	48.8 ± 0.91	48.8 ± 0.47	48.3 ± 0.34
σ_{z0}	43.3 ± 0.53	43.7 ± 0.29	43.6 ± 0.25

6.6 Case of both thin and thick discs

Fig. 6 and Table 3 show results for the more realistic case of two discs with realistic velocity dispersions. In all three cases the catalogue contained 10 000 stars and 100 000 tori were used in the analysis.

When only proper motions are available, the correlation between σ_{r0} and σ_{z0} is now rather strong for both thin and thick discs. Adding parallaxes produces a more dramatic improvement in precision than in the case of the single-disc model. Adding line-of-sight velocities also produces a material improvement in accuracy, presumably because the errors of 5 km s^{-1} in the data are a smaller fraction of typical random velocities than in the case of the pure thin-disc model. In this test the fraction of the stars in each disc was fixed at its true value. If this fraction is allowed to vary, the recovered parameters have larger uncertainties because a trade-off is possible between the velocity dispersion of the thicker com-

ponent and the fraction of the stars it carries: the lower the dispersion, the more stars it can carry. In the real world this degeneracy must be broken by using chemical information: the thick disc is fundamentally the component with high $[\alpha/\text{Fe}]$.

7 DISCUSSION

In this paper we have laid out the formalism of an approach to the interpretation of data from surveys, and have shown that it works in principle. However, we have only scratched the surface of the overall problem. Within the existing framework, we need to:

- Chart the growth in the uncertainties of the parameters as the measurement errors of the observations increase.
- Determine the precision to which the Galactic potential can be determined by fitting the potential in parallel with the DF, rather than considering it known.

The only barrier to investigating these questions is computational cost: if we change either the measurement errors or the gravitational potential, we have to re-evaluate the likelihood of the catalogue from scratch rather than by re-using the saved contributions of each torus to each star. The second of the questions above is of particular interest because upon its answer depends the prospects for pinning down the Galaxy’s dark-matter density to good precision.

The computational cost of evaluating the likelihood of a catalogue is dominated by the integrals of sight-lines in equation (21). Since there is no dependence between these integrals for different stars, the computation is parallelisable, and we do employ multiple cores.

Two other directions requiring urgent exploration are:

- Extend the formalism to models that possess more than one stellar population, each population being characterised by its own DF and distribution in the colour–luminosity plane.
- Extend the formalism to include additional observables, such as colour indices, measures of $[\text{Fe}/\text{H}]$, $[\alpha/\text{Fe}]$, etc.

The first of these directions is conceptually straightforward and not especially computationally costly. It is mandatory in the sense that it would introduce correlations between kinematics, chemistry and the luminosity function that were first identified in the Galaxy over half a century ago. Operationally it is easy: one simply takes the DF to be a superposition of DFs with a different colour–luminosity distribution for each component DF. The presence of more than one population in the system should sharpen our ability to constrain the gravitational potential from a given catalogue as it does in the simpler context of dwarf spheroidal galaxies (Amorisco & Evans 2011).

One could extend the range of observables considered in a trivial way, but at some point it becomes sensible to widen the scope of the scheme to include both a model of the chemical evolution of the Galaxy and the strong constraints on stellar parameters yielded by the theory stellar evolution. We hope to publish details of such a formalism shortly. The scope of the exercise is then broadened to diagnosing the history of the Galaxy as well as its present state,

and the resulting constraints on DF and gravitational potential would reflect the information regarding stellar distances that is normally embodied in “photometric distances”.

An issue that must at some point be addressed is:

- The impact of using an inappropriate form of the DF.

The DF of the Galaxy certainly does not consist of a superposition of the quasi-isothermal DFs we have employed here, and the question arises as to how accurately the real DF can be represented by our functional form (or some other tractable form). That is, once we have found the best-fitting DF of our form, we want to answer the question “is our catalogue statistically consistent with being drawn from the chosen DF.” At an elementary level this question is readily addressed by drawing pseudo-catalogues from the model DF and for each such catalogue calculating L from equation (18) – if the value of L obtained from the real catalogue lies within the range of those obtained for the pseudo-catalogues, then the model DF is clearly consistent with the data. In reality this exercise will always reveal that L for the real catalogue lies outside the range defined by the pseudo-catalogues, because the Galaxy is an extremely complicated system, full of structure that is not included in the model DF. Before we can pass judgement on our fitted DF we have to understand what it fails to represent: are there large-scale discrepancies between the predictions of the DF and the observations, or does it merely fail to include small-scale fluctuations that one is not endeavouring to represent at this level? Given the limitations on binning the real catalogue that were described in Section 4.2, addressing this question will be hard.

An issue in this area that can be more easily addressed is “what impact the use of an inappropriate form of the DF will have on the inferred gravitational potential and dark-matter density.” We have to expect that an inappropriate form of the DF will distort our perception of the gravitational potential because when the DF is wrong, we cannot expect the likelihood of the data to be maximised by the true potential. Clearly an erroneous potential will yield an erroneous dark-matter distribution. This question could be rigorously addressed by drawing catalogues from N-body simulations and comparing the potential and dark-matter densities inferred from the catalogue with the real ones.

A final topic that merits discussion is

- Optimising the design of surveys

Large resources are currently being invested in surveying the Galaxy, and in principle it would be useful before committing these resources to determine the most cost-effective strategy by asking questions such as “is it more useful to measure N line-of-sight velocities with errors of 5 km s^{-1} or $N/2$ velocities with errors of 3 km s^{-1} ? “Would it be more useful to increase by half a magnitude the magnitude limit of a satellite’s parallax measurements, or to measure line-of-sight velocities for a tenth of the stars? The methods described in this paper make it possible to compute precise answers to such questions.

In this context an obvious step to take now is to investigate the degeneracies between the various parameters of Galaxy models, and ask which combination of data types is most effective at breaking such degeneracies. In this paper we varied only the velocity scales of the DF. Ideally we

would also vary the other parameters in the DF, such as the scale lengths R_d and the relative normalisations of the thin and thick discs, and also the parameters of the gravitational potential, the Sun’s velocity, etc. The extent to which there are degeneracies between these parameters, will depend on the richness of the data, and it behoves us to understand the relative power of different data sets before we design a survey.

8 CONCLUSIONS

It seems inevitable that we will extract the promised science from current and upcoming surveys of the Galaxy by comparing the surveys’ catalogues with models that have been “observed” with biases matched to those of the surveys. A major goal of the surveys is to map the Galaxy’s dark-matter distribution, which is possible only in so far as the Galaxy can be presumed to be in a steady state. Consequently equilibrium dynamical models are of particular importance.

The number of variables that are commonly measured for each star is large – in addition to six phase-space coordinates and the apparent magnitude, one or more colours, the effective temperature, the surface gravity and two measures of metallicity are routinely measured because our ambitions to unravel the star-formation and metal-enrichment histories of the Galaxy turn on the availability of such data for millions of stars. In Section 4.2 we saw that even if such data were available for a billion stars, only the crudest estimate of the density of stars in the high-dimensional data space could be obtained by binning the data. Therefore it seems inevitable that models will have to be fitted to the data by maximising the likelihood of the data given a model.

These likelihoods can be calculated only if we have the pdf of the model in data space. This requirement is a major difficulty for N-body models, for which it is in principle no easier to determine the pdf than it is for the Galaxy.

For these reasons we believe models based on analytic DFs and orbital tori have unique potential for the scientific exploitation of large surveys of the Galaxy. In Section 6.4 we described how to produce a discrete realisation from a torus model, and we have made extensive use of such realisations in our tests.

In Section 4 we developed the formalism required to determine likelihoods for a torus model under some simplifications. The principal simplification was the neglect of all variables other than sky position, space velocities and apparent magnitude. Since in this framework there is no possibility of distinguishing different types of stars, for example metal-poor ones, or α -enhanced ones or constrain the age of a star, this level of analysis is only appropriate for a Galaxy that consists of a single stellar population. Therefore, this exercise is an artificial one, but nonetheless a vital one from which we can build towards work of greater complexity and realism.

The key equation (18) expresses the log-likelihood as a sum of integrals down the line-of-sight through individual tori. Since a large number of tori must be used if unbiased results are to be obtained, the computational cost of these integrals is large. Fortunately, once they have been evaluated for a given catalogue and gravitational potential, the likelihood of the data given any DF can be quickly computed.

Therefore the optimisation of the DF in a given potential is straightforward.

In Section 6 we tested the algorithm by using it to reconstruct the DF from catalogues containing either 5000 or 10000 stars with Gaia-like errors. We found that it performed as expected. The irreducible statistical uncertainty in the DF scales roughly inversely with the square root of the number of stars in the catalogue, and for 5000 stars amounts to ~ 0.5 per cent on the velocity dispersions, which is ~ 50 per cent of the uncertainty on the DF found with only measurements of the proper motion (with Gaia-like uncertainties). By adding Gaia-like measurements of parallax for 5000 stars to those of proper motion, one can drive the uncertainty in the DF almost down to the irreducible statistical uncertainty.

The uncertainties quoted above are remarkably small given the small sizes of the catalogues analysed. The uncertainties will grow, probably significantly, when the potential is varied alongside the DF. They will also grow with the sophistication of the DF, although one may hope that this growth will be to a large extent countered by enrichment of the data to include spectrophotometric data that must accompany any attempt to decompose the Galaxy into several populations with distinct DFs.

The uncertainties on parameters that we recover include the effects of measurement errors and statistical uncertainty arising from the finite number of stars in the analysed catalogue, but do not make allowance for the use of only a finite number of tori. An insufficient supply of tori will lead to biases in the results. The entropy of the probability distribution defined by equation (24) being small is a sure sign that too few tori are being used, but the surest check that enough tori are being used is to draw a fresh sample of tori from the final DF and to re-determine the pdf of the DF’s parameters using these tori. If the pdf differs materially from the original one, more tori are required.

It is remarkable that the DF can be recovered from proper motions alone because with the broad luminosity function used here the data by themselves contain negligible distance information. The distance information that is required to pin down the DF and thus establish the typical velocities of stars is provided by the gravitational potential, which sets a scale-height at any velocity dispersion, and by the solar motion through the logic of traditional secular parallaxes. Since only limited distance information is available when the data are restricted to proper motions, the two velocity scales of the DF, σ_{r0} and σ_{z0} have correlated errors.

Adding parallaxes to the data set eliminates this correlation as well as diminishing the scale of the uncertainties. Further adding line-of-sight velocities with uncertainties of 5 km s^{-1} has at most a small impact on the results.

In Section 7 we discussed several directions for further work. One urgent step is to extend the formalism to include the spectral characteristics of stars, such as metallicity, colour, effective temperature and surface gravity. The main issue here is how best to extend our models to predict their distributions. There is more than one way that this can be done, so we reserve this topic for a future paper. A related issue is how best to combine constraints from different surveys, for example an astrometric survey such as Gaia with a spectroscopic one such as the ESO-Gaia survey. One option is to analyse the catalogues one after the other,

using constraints obtained from the first analysis to define the prior used in the second analysis. Alternatively it may be possible to refine the definition of the selection function $\phi(\mathbf{J})$ in such a way that catalogues with different selection criteria can be analysed simultaneously.

In this paper we have neglected extinction. Given a three-dimensional model of the interstellar medium, it would be straightforward if computationally costly, to allow for reddening and extinction. Ideally, the model of the ISM would be refined in parallel with the Galaxy model, but it is not yet apparent how this could be accomplished in practice.

A key topic is the extent to which the Galaxy's gravitational potential can be constrained by various bodies of data. In principle this is a trivial extension of the present work, but it is computationally expensive.

Computational cost is a real issue. The cost of analysing a catalogue is proportional to the number of its stars times the mean number of tori \bar{n}_* that might make a non-negligible contribution to each star's probability. Although the total number of tori needed increases with the precision of the data, \bar{n}_* should be roughly constant between catalogues, so computational cost should scale with the number of stars in the catalogue. However, this situation may be improved by binning stars by position on the sky, and evaluating the appropriate line-of-sight integral (eq. 21) simultaneously for all the stars in a bin for a given torus, under the approximation that their position on the sky is that of the centre of the bin. Approaches like this which reduce computational effort are likely to prove essential in scaling up this algorithm from working with the pseudo-catalogues of 10 000 stars used here to analysing surveys such as RAVE, with $\lesssim 500\,000$ stars observed and, looking further ahead, the $\sim 10^9$ stars in the Gaia catalogue.

REFERENCES

- Abazajian K., et al., 2009, *ApJS*, 182, 543–558
 Amorisco N.C., Evans N.W., 2011, *MNRAS* accepted, arXiv:1106.1062
 Bahcall J.N., Soneira R.M., 1984, *ApJS*, 55, 67
 Bell E.F. et al., 2008, *ApJ*, 680, 295
 Binney J., 2010, *MNRAS*, 401, 2318
 Binney J., Dowrick N., Fisher A., Newman M.E.J., 1992 “The Theory of Critical Phenomena”, Oxford University Press, Oxford
 Binney J., Lacey C., 1988, *MNRAS*, 230, 597
 Binney J., McMillan P., 2011, *MNRAS*, 413, 1889
 Binney J., Merrifield M., 1998, “Galactic Astronomy”, Princeton University Press, Princeton
 Binney J., Tremaine S., 2008, “Galactic Dynamics”, Princeton University Press, Princeton
 Bissantz N., Debattista V.P., Gerhard O., 2004, *ApJ*, 601, L155
 Brown A.G.A., Velázquez H.M., Aguilar L.A., 2005, *MNRAS*, 359, 1287
 Carlberg R.G., Sellwood J.A., 1985, *ApJ*, 292, 79
 Dehnen W., 2009, *MNRAS*, 395, 1079
 Dehnen W., Binney J., 1998, *MNRAS*, 298, 387
 de Lorenzi F., Debattista V.P., Gerhard O., Sambhus N., 2007, *MNRAS*, 376, 71

- Epchtein N., Simon G., Borsenberger J., de Batz B., Tanguy F., Begon S., Texier P., Derrière S., and the DENIS Consortium, 2005, “DENIS Catalogue third data release” <http://cdsweb.u-strasbg.fr/denis.html>
 Eyre A., Binney J., 2011, *MNRAS*, 413, 1852
 Gebhardt, K. et al, 2003, *ApJ*, 583, 92
 Holmberg J., Nordström B., Andersen J., 2007, *A&A* 475, 519
 Kaasalainen M., 1994, *MNRAS*, 268, 1041
 Kaiser N. et al., 2002, “Society of Photo-Optical Instrumentation Engineers (SPIE) Conference Series”, 4836, 154
 Krajnović D., Cappellari M., Emsellem E., McDermid R.M., de Zeeuw P.T., 2005, *MNRAS*, 357, 1113
 Martinez-Valpuesta I., Gerhard O., 2011, *ApJ*, 734, L20
 May A., Binney J., 1986, *MNRAS*, 221, 857
 McMillan P., 2011, *MNRAS*, 414, 2446
 McMillan, P., Binney J., 2008, *MNRAS*, 390, 429
 Navarro J., Frenk C.S., White S.D.M., 1996, *ApJ*, 462, 563
 Nordström B., Mayor M., Andersen J., Holmberg J., Pont F., Jørgensen B.R., Olsen E.H., Udry S., Mowlavi N., 2004, *A&A*, 418, 989
 Perryman M.A.C., 1997, “The Hipparcos and Tycho Catalogues”, (Noordwijk: ESA Publications)
 Ratnatunga K.U., Bahcall J.N., Casertano S., 1989, *ApJ*, 339, 106
 Robin A.C., Reylé C., Derrière S., Picaud, S., 2003, *A&A*, 409, 523
 Roman N.G., 1954, *AJ*, 59, 307
 Schönrich R., Binney J., 2009, *MNRAS*, 399, 1145
 Schönrich R., Binney J., 2011, *MNRAS*, accepted, arXiv:1109.4417
 Schönrich R., Binney J. & Dehnen W., 2010, *MNRAS*, 403, 1829
 Sharma S., Bland-Hawthorn J., Johnston K.V., Binney J., 2011, *ApJ*, 730 3
 Skrutskie M.F., et al., 2006, *AJ*, 131, 1163
 Schwarzschild M., 1979, *ApJ*, 232, 236
 Siebert A., et al., 2011, *AJ*, 141, 187
 Simon R., Brook C.B., Martel H., Kawata D., Gibson B.K., Sanchez-Blazquez P., 2010, *MNRAS*, 402, 1489
 Spitzer L., Schwarzschild M., 1953, *ApJ*, 118, 106
 Steinmetz M., et al., 2006, *AJ*, 132, 1645
 Syer D., Tremaine S., 1996, *MNRAS*, 282, 223
 Yanny B., et al., 2009, *AJ*, 137, 4377
 Zacharias N., et al., 2010, *AJ*, 139, 2184

APPENDIX: PROOF THAT L IS STATIONARY FOR THE TRUE DF

By the Monte-Carlo integration theorem, the sum over α in the definition (18) of the likelihood L can be replaced by an integral over \mathbf{u} times the pdf of the stars in that space, which is $\text{Pr}_o(\mathbf{u}|f_t)$, where f_t is the true DF. Hence

$$L = \int d^7\mathbf{u} \text{Pr}_o(\mathbf{u}|f_t) \ln[\text{Pr}_o(\mathbf{u}|f)], \quad (30)$$

so

$$\frac{\partial L}{\partial a} = \int d^7\mathbf{u} \text{Pr}_o(\mathbf{u}|f_t) \frac{\partial \text{Pr}_o(\mathbf{u}|f)/\partial a}{\text{Pr}_o(\mathbf{u}|f)}. \quad (31)$$

When $f = f_t$ the denominator cancels with the pdf on top and we find

$$\left. \frac{\partial L}{\partial a} \right|_{f=f_t} = \int d^7 \mathbf{u} \frac{\partial \text{Pr}_o(\mathbf{u}|f_t)}{\partial a}. \quad (32)$$

This vanishes because it is the derivative of $\int d^7 \mathbf{u} \text{Pr}_o(\mathbf{u}|f_t) = 1$.